Iranian Journal of Pharmaceutical Sciences
Spring 2008: 4(2): 135-140
www.ijps.ir

Original Article

Crystallization Kinetics of Hydroxyapatite Nano-films on Stainless Steel Through a Sol-Gel Process

Hossein Najafi[a,*], Ziarat Ali Nemati[a], Zahra Sadeghian[b], Nafiseh Sohrabi[a]

[a]*Department of Materials Science and Engineering , Sharif University of Technology, Tehran, Iran,*
[b]*Oil Research Center, Tehran, Iran*

Abstract

This article describes the preparation and analysis of nano hydroxyapatite (HA) films on stainless steel 316L through sol-gel technique. The process started with preparation of a nitrate and phosphate sol. After aging the sol for 24 h at room temperature a SS316 substrate was dip-coated and heat-treated at 350 to 450 °C for different times in air. The coating phase and structure on substrate were investigated by X-ray diffraction (XRD), fourier transform infrared (FT-IR), differential thermal analysis (DTA) and scanning electron microscopy (SEM). Degree of crystallinity and time temperature transformation (TTT) diagram of HA films obtained with using Avrami equation. Results indicated that HA phase began to crystallize after a heat treatment at 250 °C and the crystallinity increased at a temperature of 450 °C. The HA film showed a nano structure with suitable crystallinity after heat treatment.

Keywords: Crystalization; Dip-coating; Nano hydroxyapatite; Sol-gel.
Received: December 7, 2007; *Accepted:* February 12, 2008

1. Introdution

Because the main role of bone implants that used for reconstruction of bone defects, they should exhibit high biocompatibility and bioactivity as well as very good mechanical properties. Among the implant materials that are applied nowadays, no one has the requirements defined for implants [1]. Due to the chemical similarity between hydroxyapatite (HA) and mineralized bone of human tissue, this material exhibits strong affinity to the bone. The basis of this process is formation of good chemical bond between HA and bone. However, poor mechanical properties of HA restrict its practical applications.

Nowadays, HA coatings on metallic substrates offer great improvement in orthopedic and dental applications. This composite system including HA coatings on metallic implants is produced a composition of good mechanical properties of metallic substrate and bioactivity surface properties for HA biomaterial [2]. In general, existence of HA coatings on metallic implants have advantages such as biocompatibility, encouraging of cellular reproduction and prevention of toxic ion entry to body environment [3].

While the plasma spray method is most

*Corresponding author: Hossein Najafi, Department of Materials Science and Engineering, Sharif University of Technology, Tehran, Iran.
Tel (+98)21-66165240
E-mail: hnajafi@mehr.sharif.edu

commonly used to coat metallic implants [4], this method has been associated with adhesive failure and also it is difficult to modify the microstructure of the coatings to achieve optimum response in the body.

The sol-gel method is an alternative means to form coatings, and has several advantages [5]. First, the microstructure of solids obtained using sol-gel techniques can be modified by changing the chemistry and processing conditions. In addition, thin films of uniform thickness can be made using sol-gel process [6]. One of the important properties of HA coatings is the degree of crystallinity that has important effect on the mechanical properties [7]. In this study, HA coatings with different conditions of heat treatment have been examined. The main objective of this work is to introduce the time temperature transformation (TTT) diagram of HA to obtain the full crystallinity. TTT diagrams have been used to find the optimum processing path. In addition, a recurring goal was to determine the factors controlling HA crystallization in sol-gel systems.

2. Materials and methods

Raw materials for preparation of solutions are $Ca(NO_3)_2.4H_2O$ and $(NH_4)_2HPO_4$. At first, $Ca(NO_3)_2.4H_2O$ (99% pure, Merck, Darmstadt, Germany) is dissolved in 50 ml deionized water at 40 °C and then is added with a very slowly rate inside solution that is containing 50 ml deionized water and $(NH_4)_2HPO_4$ (99% pure, Merck) by stirring. Concentration of solutions is selected such that Ca/P will be 1.67. pH of the solution before and after stirring is considered above 9.1% W ammonium polyacrylate (NH_4PAA) is used as dispersant for providing stable solution and nano-morphology. This solution was stirring 90 min. and aged in ambient environment for 24 h. The second stage is preparation of 316 L stainless steel samples that their dimensions at this stage was 20mm×10mm×2mm. Samples were surface sandblasted by SiC for removing surface impurities then washed with acetone and distillated water and substrates were dip coated with the solution by a withdraw speed of 5 cm/min. (Figure 1). The coatings were then dried at 80 °C followed by heat treating in air for 50, 100, 200, 500 and 1000 seconds. Analysis of coatings was done by differential thermal analysis (DTA), X-ray diffraction (XRD), fourier transform infrared (FT-IR) and scanning electron microscopy (SEM). Determination of crystallinity reasonable temperature and time for crystallization process of coating by Avrami equation and drawing of TTT diagram is done [6-8].

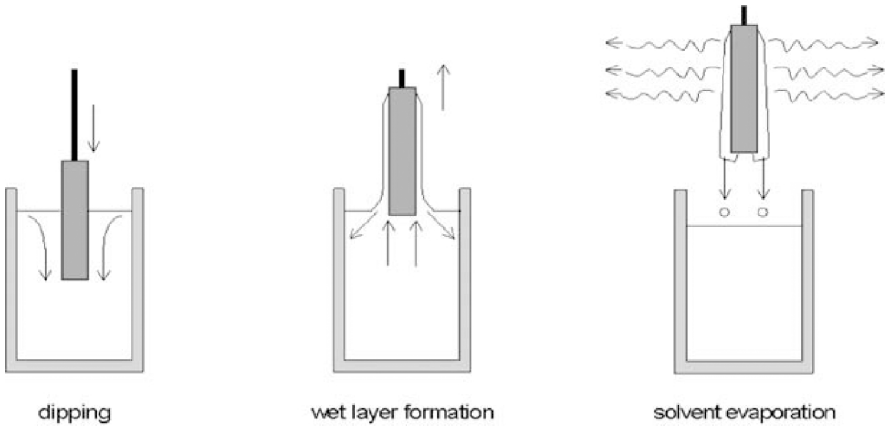

Figure 1. Stages of the dip coating process: Dipping of the substrate in to the coating solution, wet layer formation by withdrawing the substrate and gelation of the layer by solvent evaporation.

3. Results

3.1. DTA analysis

Figure 2 shows the DTA analysis. DTA curve indicated an endothermic peak at 102 °C and an exothermic peak at 250 °C. Above 400 °C the curve has no obvious changes. The endothermic reaction at 102 °C was believed to be related to the evaporation of residual adsorbed water, and another reaction at 250 °C with exothermic peak was thought to arise from the crystallization of HA [9].

3.1.1. A. XRD analysis

The XRD patterns of the standard HA and coating are shown in Figure 3. For isothermal process at 350 °C in different times, we have an important peak at 31.8 that is related to apatite phase. Difference between intensity and clearance of peaks at different times, shows that formation of apatite phases in more times is completed Figure 3 is considerable for processes in 400 and 450 °C. Synthesis of HA at low temperature causes that undesirable phases like tricalcium phosphates can't produce, that are formed at higher temperatures besides HA. As seen peaks that are relative to these phases don't exist.

The crystallinity was evaluated from the main peak ratio base on a relative method,

Table 1. Determination of n and k constants for isothermal processes.

Isothermal temperature	n	k
350 °C	0.39	0.13
400 °C	0.42	0.15
450 °C	0.42	0.20

where 'I' is the main peak height of HA on the XRD pattern of the coating and IHA is the main peak height of HA on the XRD pattern of the powder [10]. The HA powder considered as a material of 100% crystallinity (Figure 4). The degree of crystallinity (DOC) was defined as follows:

$$DOC(\%) = I/I_{HA} \times 100 \qquad \text{Equation (1)}$$

In the next stage with uses Avrami equation TTT diagram of coatings crystallization is drawn (Figure 5). The Avrami equation, shown below, was used to model the isothermal growth data [10]:

$$x = 1 - \exp(-kt^n) \qquad \text{Equation (2)}$$

Where 'x' is the crystallization percentage 't' is the soaking time, and 'n' and 'k' are fitting constants. The values of n and k were determined by rewriting the Avrami equation as ln(-ln(1-x))=ln(k)+nln(t), and performing a least squares fit to the isothermal growth data. The values of 'n' and 'k' determined for each curve are tabulated in Table 1.

It is evident that the characteristic "C" shape, typically found in transformation

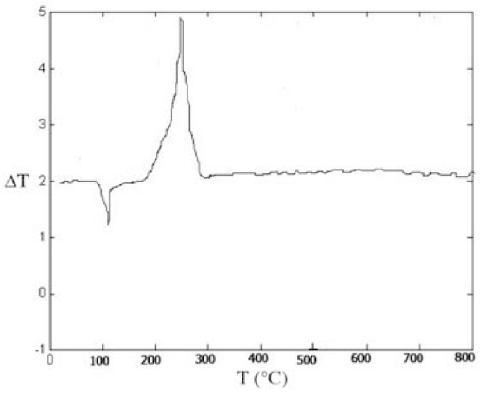

Figure 2. DTA curve of HA (exothermic peak at 250 °C).

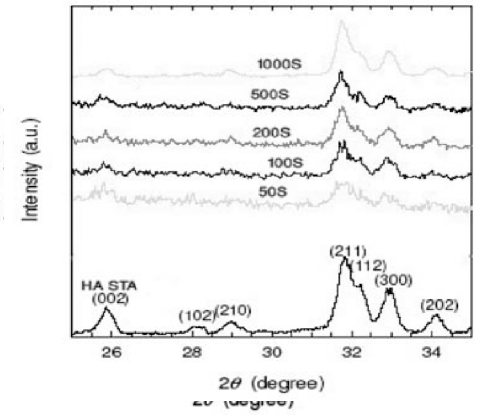

Figure 3. XRD patterns of HA coatings with different firing time.

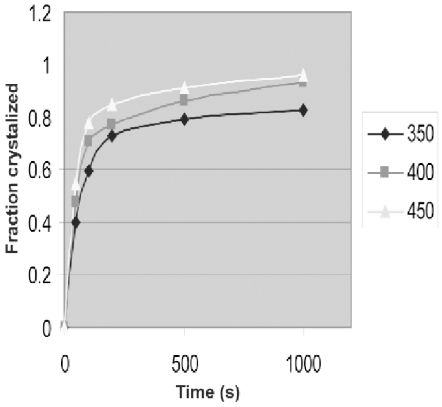

Figure 4. Isothermal growth curves corresponding to the transformation from the amorphous film to crystalline HA.The fraction crystallized is defined as the relative intensity of the (211) HA diffraction line found in the film after an isothermal anneal compared to the intensity found in fully crystallized material.

studies from a high to low temperature phase, is not observed. An explanation for this behavior can be found in the discussion section. In TTT diagram T=450 °C and t=30 min. for gaining of full crystallization are watched.

3.2. FT-IR analysis

Figure 6 shows the FTIR spectra of the annealing coatings at different temperatures that showed an OH stretching band at 3571 cm^{-1} and OH vibrational band at 630 cm^{-1} and PO_4 groups at around 550 to 630 cm^{-1} and 930 to 1100 cm^{-1}. These peaks at heating samples show apatite structure at coatings and with elevating temperature intensity and clearance of peaks will be more due to improvement crystallinity of the coated HA layer and obtain a homogeneous surface layer.

3.3. HA coatings morphology

Figures 7-9 show electron microscopy images of HA coatings that are heat-treated in different temperatures for 30 min. Average particle size will be 60 nm that with increasing the annealing temperature will increase to 120 nm. In this process, coatings will be denser with very lower microcracks in comparison with regular methods such as plasma spray. Main advantage of the sol-gel process will be reduction of coating thickness consequently reduction of the microcracks and with increasing the temperature tendency to the agglomeration of the particles will be increased.

4. Discussion

Sol-gel method for producing HA coatings is easier and has more benefits in comparison with other methods such as a lower thickness, lower working temperature and lower volume

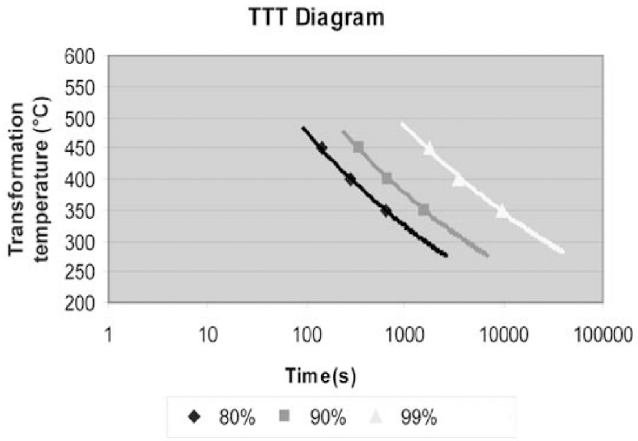

Figure 5. TTT curves of HA coating crystallization for different values.

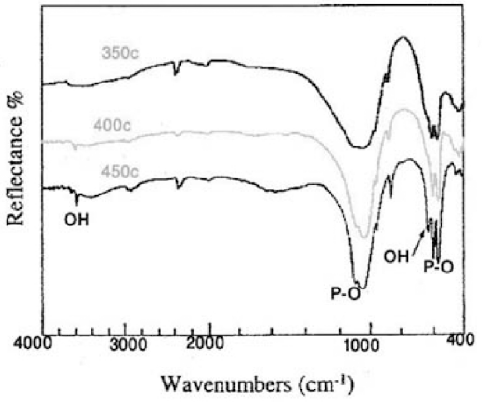

Figure 6. FT-IR analysis of coatings in different temperatures.

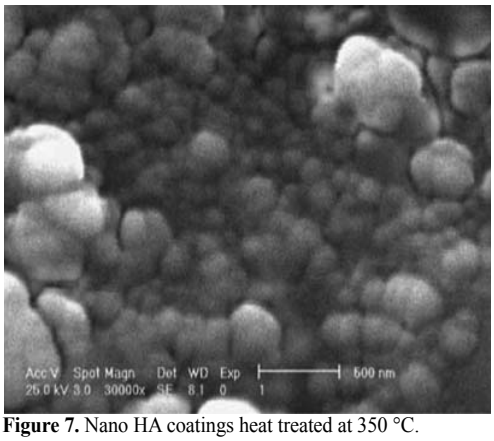

Figure 7. Nano HA coatings heat treated at 350 °C.

shrinkage. The process results in a high quality thin HA layer that imparts biological affinity to the underlying substrates for medical uses [4]. It has been suggested that the biological responses of HA coatings *in vivo* were dominantly affected by the phase purity and crystallinity of the HA-coated layer [11]. Thomas and Cook attributed the resorption of HA coatings to their low crystallinity. Therefore, as higher crystallinity of HA can be a very important factor for successful HA coating by the sol-gel process, so determination of crystallization percent and drawing of TTT diagram of HA coatings can help us improve properties [12, 13]. It was shown that the characteristic "C" shape of the TTT curve corresponding to maximum value of the crystallization rate was absent. The "C" shape curve of TTT diagrams, generally seen in the transformation from the liquid to solid phase, is due to the existence of tow competing mechanisms: (1) increasing the degree of under-cooling increases the driving force for crystallization, while (2) decreases the atomic mobility. The combination of these two effects leads to the existence of a temperature at which a maximum rate of crystallization occurs. When kinetic studies are performed on glasses, however, the initial state of the materials corresponds to a degree of under- cooling very much higher than that found in systems taken from the melt. HA has a melting temperature of 1550 °C, and thus the amount of under-cooling at a firing temperature of 450 °C is 1100 °C. The limiting factor in forming crystalline HA is thus the atomic mobility, and increasing the firing temperature, therefore,

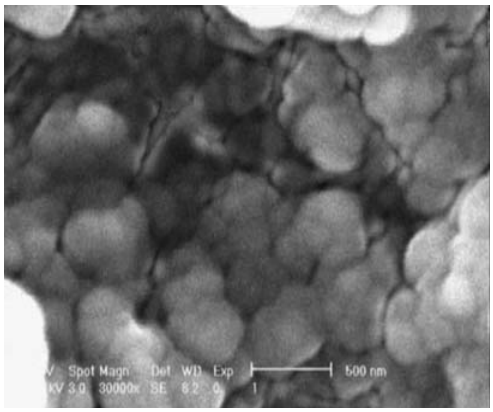

Figure 8. Nano HA coatings heat treated at 350 °C.

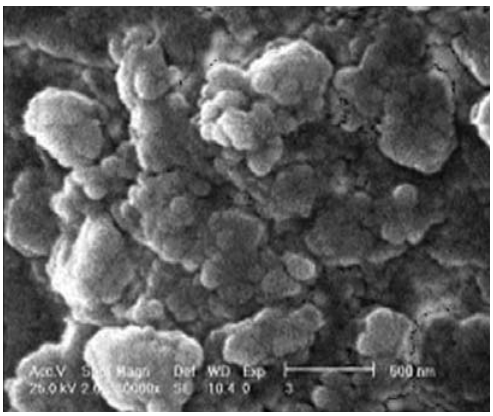

Figure 9. Nano HA coatings heat treated at 400 °C.

leads to a monotonic increase in the crystallization rate [12, 13]. As a general statement on the use of Avrami formalism to describe the extent of crystallization transformation, it should be noted that determination of the value of n does not uniquely determine the mode of transformation. This value depends on the nature of both the nucleation and growth processes.

From a mechanical point of view, nanoparticles produce better mechanical bond with metallic surface. By producing nanostructure, nucleation and growing of microcracks decreases so fracture toughness of nano HA structure increases. Stainless steel 316L in comparison with Ti alloys produce many lower chemical bonds with apatite phase and strength of coating influences mechanical bond, so producing nanostructure in HA coatings on SS316L is important. Other benefits of nanostructure in apatite coatings are for lower annealing temperature, we have lower undesirable phase transformation in coating and base metal.

4. Conclusion

Formation of HA coatings with nanostructure on 316L stainless steel by sol-gel method was considered. Crystallization of these coatings that have important role in their properties was studied by TTT diagrams. The Avrami formalism was used to describe the rate of crystallization. The formation of crystalline HA was found to be very rapid at temperatures above 400 °C. Low temperature can prevent from producing undesired phases.

References

[1] Sarczyk ASL, Klisch M, Ewicz MBA, Piekarczyk J, Stobierski L, Kmita A. Hot pressed hydroxyapatite-carbon fibre composites. *J Euro Ceramic Society* 2000; 20: 1397-402.

[2] Liu DM, Troczynski T, Tseng WJ. Water-based sol-gel synthesis of hydroxyapatite. *Process Develop Biomater* 2001; 13: 1721-30.

[3] Hench LL, Wilson JO. *An introduction to bioceramics*. Vol. 1. Florida: World Scientific Publishing Company, 1993.

[4] Liu DM, Chuou HM, Wu JD. Plasma-Sprayed hydroxyapalitic coatings: Effect of diffrent calcium phosphate ceramics. *J Mater Sci Mater Med* 1994; pp; 147-53.

[5] Brinker CJ, Scherer GW. *Sol-gel science*. Boston: Academic Press Inc., 1990.

[6] Mavis B, Cuneyt A. Dip coating of calcium hydroxyapatite on Ti-6Al-4V Substrates. *J Am Cer Soc* 2000; 83: 989-91.

[7] Sadeghian Z, Heinrich JG, Moztarzadeh F. Influence of powder pre-treatments and milling on dispersion ability of aqueous hydroxyapatite-based suspensions. *Ceramics Inter* 2006; 32: 331-7.

[8] Liu DM, Yang Q, Troczynski T. Sol-gel hydroxyapatite coatings on stainless steel substrates. *Biomaterials 2002*; 23: 691-8.

[9] Ducheyne P, Raemdonck WV, Heughebaert JC, Heughbaert M. Structural analysis of hydroxyapatite coating on titanium. *Biomaterial* 1986; 7: 97-103.

[10] Balamurugan A, Balossier G, Kanna S, Rajeswari S. Elaboration of sol-gel derived apatite films on surgical grade stainless steel for biomedical applications. *Materials Lett* 2006; 60; 2288-93.

[11] Weng W, Baptista JL. Sol-gel derived poroushydroxyapatite coatings. *J Mater Sci Mater Med* 1998; 9; 159-63.

[12] You C, Oh S, Kim S. Influences of heating condition and substrate surface roughness on the characterstics of sol-gel derived hydroxyapatite. *J Sol-gel Sci & Technol* 2001; 21; 49-54.

[13] Porter DA, Easterling KF. *Phase transformations in metals and alloys*. Boca Raton: CRC Press, 1980.

[14] Lopatin CM, Pizziconi VB, Alford TI. Crystallization kinetics of sol-gel derived hyporxapatite thin films. *J Matter Sci-Matter Med* 2001; 12: 767.